Industrial DC Microgrid Analysis Through Linear Power Flow

***Abstract*—The energy shift towards renewable energies have brought an increased interest into DC microgrids as a decentralized option with increased efficiency and easier control that can facilitate this transition.Many efforts have been made into the optimization and planing of these proposed DC microgrids. In this paper, the author proposes an approach in which a planned DC microgrid can be simulated through the use of linear power flow. This approach allows to study the evolution of the steady state of the microgrid over time. The proposed method allows to simulate the contributions and limits of batteries, and to obtain the voltages, the currents, and power injections at each time step. With these results, the expected performance and benefits of a DC industrial microgrid can be assessed. The simulation results obtained using Python showcase the results and insights obtainable with the proposed approach.**

***Index Terms*—DC power flow, DC microgrid**

I. Introduction

In recent years, microgrids have been gathering interest due to their de-centralized characteristics and their ability to aid in the incorporation of renewable energy sources such as photovoltaics (PVs). At the same time, the study of DC microgrids has been increasing due to their possible advantages such as needing less power conversions and reduced line losses when compared to their AC counterparts. DC microgrids also present a reduced system complexity due to the absence of reactive power and absence of a need for frequency synchronization [1].

In the context of the energy transition, industries are faced with new challenges. Some of these are the need to limit their carbon emissions through a shift to renewable energies, and the need to limit their power consumption from the main grid. This last one being linked to the increasing energy prices in Europe. From this perspective the adoption of PVs and batteries that complement the production profile of the PVs is interesting for the industrial consumers. As these technologies would allow them to decarbonize their energy and to reduce their energy consumption from the grid. The adoption of a DC microgrid allows to maximize these gains. The interconnection among industrial consumers would allow to increase their reliability, and reduce the amount of energy needed from the main grid. This is due to the different consumption profiles that allow for the sharing of produced or stored energy in a complementary fashion.

As described in [2], the planning of a microgrid is a complex problem that involves several costs such as the cost of investment, cost of planning, cost of maintenance and cost of reliability. Such a complex problem has been the subject of many studies. In [3], an overview of the work done regarding the planing of microgrids is given. This also includes different methods for sizing of the energy storage systems (ESS) which is a complex problem itself.

In this paper a methodology for simulating a planned DC microgrid is developed. The proposed analysis method takes the planned capacity for the ESS and PVs, and uses it in conjunction with the consumption profile of the microgrid members. For example, the metering data sampled every 15 minutes can be used to get a representation of the consumption profile of the microgrid members. Using this data along with the irradiance data for the simulated area allow to study a plausible performance of the microgrid.

At each time step, the load demand and power generation capabilities of each microgrid member are taken into account to calculate a linear power flow as developed in [4]. The linear load flow allows for an accurate simulation of the DC microgrid while providing a fast computation time. The results of the power flow are then taken into account for the next time step. In [5], the author adapted the previously mentioned linear power flow for bipolar DC microgrids. The approach described in this paper can also be applied for bipolar DC microgrids by using the bipolar linear power flow method.

The approach to be described allows to study the evolution of the values of the voltages, the currents, and the power injections in the microgrid with each data time step. The resulting data can be used to asses the expected maximum current values and the most significant voltage dips. Additionally, the saved energy linked to the energy sharing among the different members of the microgrid can be calculated. From the obtained data two important metrics can be calculated. These are the self consumption index (SCI) and the self sufficiency index (SSI). These two can be used to gain further insight of the performance of the proposed DC industrial microgrid.

The paper is organized as follows. Section II briefly presents the linearised power flow which is used for the power flow calculation in each time step. Section II describes the iterative process used for simulating the DC microgrid. In section IV, the calculation of the SCI and SSI is presented. Section V presents the configuration of the simulated DC microgrid used and the obtained results. Finally, the conclusion is given in section VI.

II. Linearised Power flow

A power flow is an essential tool that provides a view of the steady state voltages, power injections, and line flows of the system. The existing AC microgrids power flow methods can not be directly applied to the DC microgrids mainly because the AC power flow methods do not reflect the steady state characteristics of a DC system. This is due to the possible absence of a slack bus, and the fact that power injections for droop controlled generators vary with voltage, and thus they cannot be specified apriori [4]. In this section the used linear DC power flow is briefly described.

The linearised method allows the modeling of nodes that can simultaneously contain droop controlled dispatchable generators, non-dispatchable generators, and different type of loads in the power flow. Additionally, it avoids the usage of iterative techniques like the Newton-Raphson method or the trust region method. Since it relies on solving linear equations, it does not require the computation of the Jacobian matrix thus providing a faster technique. The power flow can be solved in a single iteration unless power limits are imposed to the dispatchable generators.

To solve the power flow problem an equation for the current injection at each node is needed. Equation (1) represents the current injection at a node i in a system of NB nodes. The left hand side expresses the relationship between the node current I_{ni} and node voltages V expressed through the conductance matrix G. The right hand side of the equation is composed of three elements. The first element corresponds to the current injection due to the droop controlled generator where V_0 is the no load reference voltage and Rd_i is the droop parameter. The second one is the current injection linked to the non-dispatchable generators, and the last component is the current drawn by the constant power load.

$$I_{ni} = \sum_{j=1;j\neq i}^{NB} G_{ij}V_j + G_{ii}V_i = \frac{V_{0i} - V_i}{Rd_i} + \frac{P_{ndgi}}{V_i} - \frac{P_{Pi}}{V_i} \quad (1)$$

Equation (1) is not linear due to the V_i terms found at the denominator of the elements corresponding to the non-dispatchable generator and the constant power load. In order to linearise the system, the node voltages are expressed in per unit. If expressed in per unit, the node voltage can be described in terms of the voltage deviation ΔV_i.

$$V_i = 1 - \Delta V_i \quad (2)$$

In [4] by defining a function $\phi(\Delta V_i)$ and by developing the Taylor series around zero, it is found that the higher order terms can be neglected, and thus it is possible to define (2) as:

$$\frac{1}{1 - \Delta V_i} = \frac{1}{V_i} = 1 + \Delta V_i = 2 - V_i \quad (3)$$

By using (3), the right side of (1) can be written as the following linear equation:

$$I_{ni} = \frac{V_{0i} - V_i}{Rd_i} + (P_{ndgi} - P_{Pi})(2 - V_i) \quad (4)$$

Thus, the system can be expressed as a set of linear equations as shown in (5). To solve the power flow, the equations can be set as a $Ax = B$ system to be solved where x is the vector of unknown voltages.

$$\begin{aligned} &\sum_{j=1;j\neq i}^{NB} G_{ij}V_j + (G_{ii} + \frac{1}{Rd_i} - P_{Pi} + P_{ndgi})V_i \\ &= \frac{V_{0i}}{Rd_i} - 2(P_{Pi} - P_{ndgi}) \end{aligned} \quad (5)$$

III. Microgrid simulation

In the simulated microgrid, there are nodes that represent the industrial consumers and one node that represents the point of connection towards the main grid. Each consumer node consists of three different elements. These are: the PV panels that are considered as non-dispatchable generators, the batteries that are considered as droop controlled generators, and the loads which act as constant power loads. The main grid node consists only of droop controlled source that has a droop value R_d that changes according the situation. When the microgrid can manage all the power injections by itself, R_d is equal to infinity. In other words, it does not participate in the energy injection. However, when the industrial microgrid sends or receives power from the main grid, the power is injected through this node. In this case the droop parameter is not equal to infinity.

To simulate the described microgrid an algorithm workflow similar to the one presented in [6] is adopted. The used algorithm workflow is presented in Fig. 1. As a first step the variables defining the microgrid such as the line resistances, droop resistances, and battery parameters are defined. The PV production data and consumption profiles are also loaded. Once the initialization stage is done, the first PV production and load demand data are selected. Afterwards, a function checks the state of charge (SoC) of the batteries. Based on the SoC and the maximum output power, the power limit P_{lim} of each battery is obtained. If there are any limits imposed on the maximum and minimum percentage of SoC, they will also be taken into account for the calculation of P_{lim}. This power limit along with the consumption and PV production data are fed into the linear power flow algorithm. How this data is used in the linear power flow is detailed in the next subsection.

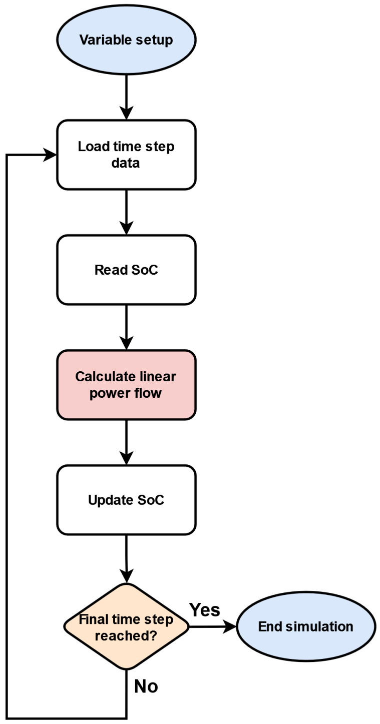

Fig. 1. DC Microgrid algorithm workflow

Once the linear power flow is calculated, the energy given by the battery is calculated. Indeed, the result of the power flow is total energy in each node. However, the energy corresponding to the PVs and the load demand at each node are known. Therefore, by adding these three quantities the energy absorbed or given by the battery can be known. The power given or absorbed by the battery is then used to update the SoC of it. This process is repeated until the last set of values is reached.

A. *Power flow implementation*

For the power flow implementation the approach described in Section II has to be expanded upon. The algorithm workflow for the calculation of the linear power flow is illustrated in Fig. 2. The first step, is the implementation the linear power flow as described in Section II. The obtained results of solving the $Ax = B$ system of equations are used to calculate the power at each node. Using the known load demand and PV production the power corresponding to the battery is calculated. This value is then compared to the power limit P_{lim}. If it is under the limits, the linear power flow algorithm can be stopped and return the found values. Otherwise, the batteries of the nodes where the power limit is exceeded are set as non-dispatchable generators. This is done by fixing their droop parameter equal to infinity and setting the non-dispatchable power P_{ndgi} equal to the sum of the power coming from the PVs and the battery P_{lim}. The parameters are then updated, and the linear power flow is allowed to iterate.

In the case that all the batteries are acting as non-dispatchable units, the node corresponding to the point of connection towards the grid is set as a grid forming node. This is achieved by setting a small value for the droop resistance R_d. The batteries will provide or store power according to their power limit P_{lim}, and the main grid node will compensate for any remaining power unbalance. Thus, in the final iteration no battery should surpass its power limit P_{lim} and the linear power flow will return the found values.

Although adding power limits requires that the system iterates, it will not significantly slow down the computation. For each time step a system of NB nodes will iterate a maximum of NB times. This is due to the main grid node becoming activated when the all the batteries are set as non-dispatchable units.

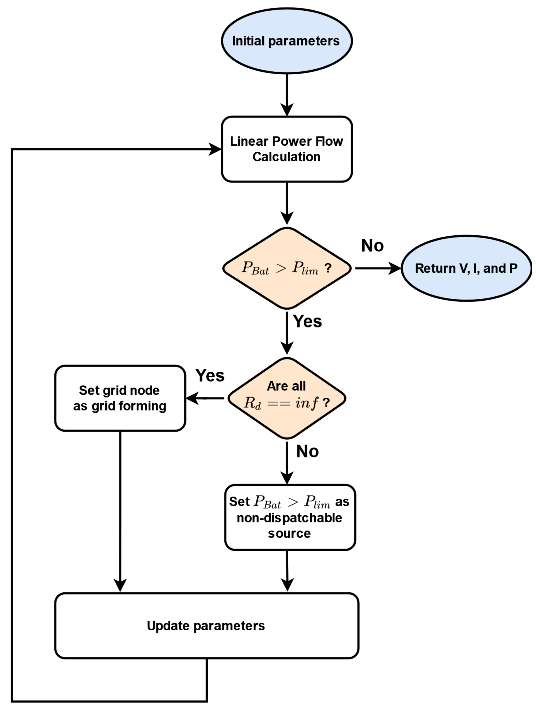

Fig. 2. DC linear power flow workflow

B. *Battery simulation*

As previously mentioned, the batteries are acting as droop controlled sources. The droop parameter for each battery is calculated using its rated power and discharge rate. The discharge rate is a measurement of how much power can the battery supply relatively to its rated capacity. For example if a 80 kWh battery can only output 40 kW at a time it has a discharge rate of 0.5. By using the previous parameters, the droop parameter can be calculated by obtaining the battery maximum output current. The droop parameter can be calculated as shown in (6) [7].

$$R_d = \frac{\varepsilon_v}{i_{max}} \tag{6}$$

Where ε_v is the maximum allowed voltage deviation, that is the percentage of allowed deviation times the nominal voltage V_0.

For updating the SoC, the coulomb counting method is used. Thus, the duration of the time step has to be taken into account as the power charged or discharged is integrated to obtain its value kWh. The obtained power in kWh is then used to update the SoC percentage before the next time step.

IV. Results

In order to showcase the proposed methodology, the DC microgrid shown in Fig. 2 is simulated. This microgrid consists of 5 nodes. The right most node is the node corresponding to the point of connection towards the main grid. The other 4 nodes represent the different industrial consumers. Each node has a constant power load, their own PV production, and a droop controlled ESS.

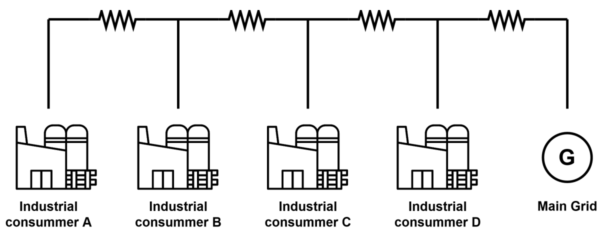

Fig. 3. Industrial DC microgrid test grid

The simulation is carried out using the consumption data sampled every 15 minutes, and it covers the duration of 10 months. It also uses historic irradiance data corresponding to the Western European region. An example of the consumption profile of the consumers in one week is shown in Fig. 4.

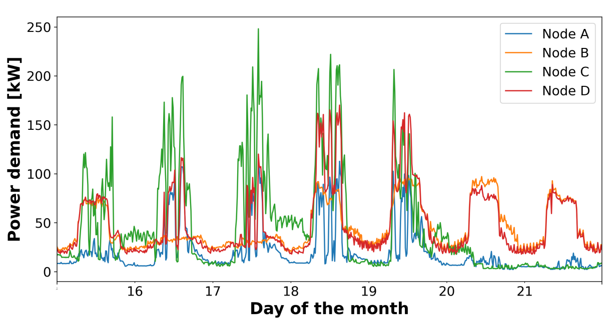

Fig. 4. Weekly consumption profile example

The battery capacity, discharge rate, droop parameter, and the PVs capacity in kWp are given in Table I. The energy demand, energy import from the grid, and the exported energy towards the grid for each industrial consumer and the ensemble is given in Table II. These energy values can be used to measure the impact on the energy imports due to the industrial microgrid. The line lengths and resistances of the microgrid are given in Table III.

TABLE I
Consumers Battery and PV Parameters

Consumer	Battery [kWh]	D rate	$R_d[\Omega]$	$P_{PV}[kWp]$
A	100	1.5	-0.0933	100.5
B	200	0.5	-0.1400	150.75
C	130	1	-0.3769	100.5
D	200	0.8	-0.3063	184.25

TABLE II
Consumers Energy Parameters

Consumer	Demand [MWh]	Import [MWh]	Export [MWh]
A	144.92	73.33	23.81
B	300.91	171.41	13.62
C	352.41	275.95	18.95
D	328.37	174.76	21.29
Total	1126.61	695.45	77.66

TABLE III
Used line parameters

Line	Length [m]	Resistance [Ω]
A to B	500	0.0321
B to C	250	0.0160
C to D	440	0.0282
D to Grid	680	0.0436

A. Industrial microgrid simulation

First, the proposed approach is used to study the possible voltage level options for the microgrid and their effect in terms of saved energy and line losses. This saved energy corresponds to energy that is given by members of the DC microgrid instead of being taken from the main grid. To do this the industrial microgrid is simulated multiple times changing the nominal voltage in each iteration. The obtained results are shown in Fig. 5. At a nominal voltage of 500 V the line losses are close to 40 MWh. As the voltage level increases the line losses start reducing. Increasing the voltage level reduces the line losses and allows to transport energy more efficiently thus increasing the saved energy as well. It is noticeable that the higher voltages have the highest amount of energy saved. on the other hand, the energy saved at 500 V is negative. This is because the gain is calculated against the total energy import from Table II which does not take line losses into account. In other words, the energy savings that could be generated by a micro-grid are lost due to the high line losses in that case.

Although higher voltage levels have a better performance in terms of line losses and energy saved, the gain between each voltage level starts becoming smaller. Moreover, a higher voltage level can have an impact in the sizing of the components, the efficiency of the power electronics, and the protection devices needed. Therefore, working for example with 1kV can be more advantageous than 1.3kV in some scenarios.

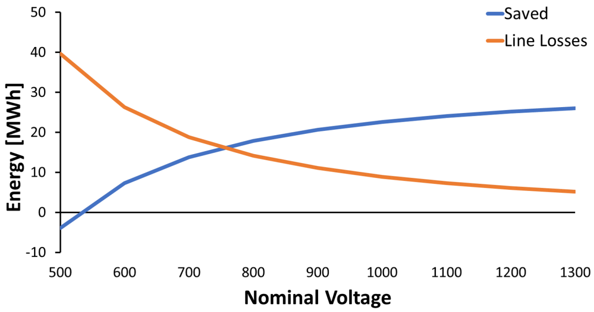

Fig. 5. Saved energy and line losses according to the nominal voltage

For this study, a nominal voltage of 1kV is used for the DC microgrid. With such nominal voltage, the results shown in Table IV are obtained. Table IV shows that the saved energy corresponds to 22.62 MWh. These 22.62 MWh are provided from the surplus power of the members of the microgrid instead of importing it from the grid. This savings correspond to 3.25% of the total energy that would be imported otherwise. This is a 3.25% of energy savings on top of the individual gains that industrial consumers can obtain by adopting the use of PVs and ESS.

TABLE IV
MICROGRID SIMULATION RESULTS

Import [MWh]	Saved [MWh]	Export [MWh]	SCI	SSI
672.83	22.62	46.29	90.78%	41.00%

Through this simulation, it is also possible to study the evolution of the voltage at each time step. Fig. 6 shows the average value of the voltage in each node in per units. It also shows the most significant voltage dips experienced at each node. It is shown that in average the voltages stay close to their nominal values. Node A has the most significant voltage dip. This fact can be linked to its relative longer distance to the main grid node. Due to the DC nature of the grid, a voltage difference between the nodes is needed to transfer the power. When all the power is supplied by the grid, the power transfer is done in a single direction from right to left. This causes the necessary voltage differences to chain together thus causing a lower voltage level at the leftmost node.

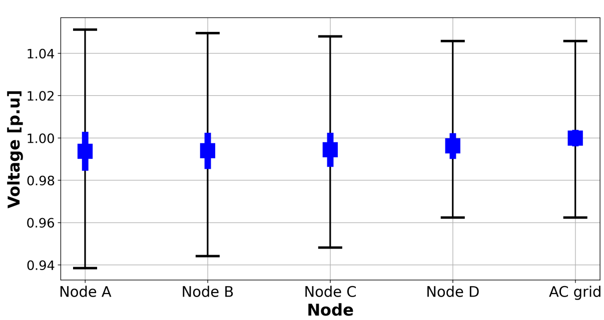

Fig. 6. Voltage statistics for each node of the DC microgrid

Through the linear loadflow performed at each time step, it is also possible to know the expected line currents at each step as well. Thus, one can record the average currents and also the maximum currents as shown in Fig. 7. In Fig. 7 it is shown that the maximum currents have a significantly higher amplitude compared to their average values. The line connecting the main grid to consumer D has the highest maximum value. This is natural as all the energy import or export has to go through this line. Thus, it can be seen that as the lines get further from the node connecting to the main grid their maximum current become lower. With this results it can be decided if the obtained currents are acceptable or if the currents have to be reduced by using a line of lower resistance. Equally, the expected line losses can be calculated with the obtained data.

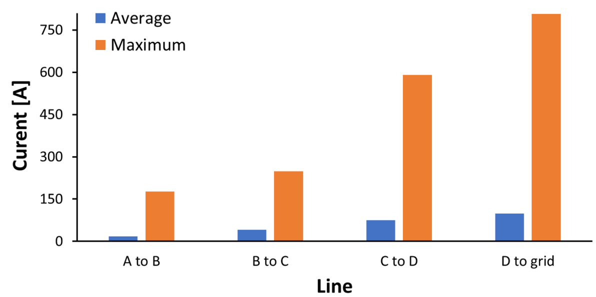

Fig. 7. Average and Maximum current at each line of the DC microgrid

B. SSI and SCI

Based on the logged data for each time step, two important metrics can be calculated. These are the self consumption index (SCI) and the self sufficiency index (SSI). According to [8], the SCI is a measurement of the PV energy that is used directly or stored in the ESS. Meanwhile, the SSI corresponds to the energy consumption that is instantly supplied either by the PVs or the ESS. The calculation of the SCI and SSI has been adapted from [8] as follows:

$$SCI = \sum \frac{min(P_v, P_{load} + P_{charge})}{\sum P_v} \quad (7)$$

$$SSI = \sum \frac{min(P_{load}, P_v + P_{discharge})}{\sum P_{load}} \quad (8)$$

As it was shown in Table IV. The obtained SCI and SSI are 90.78% and 41% respectively. This high SCI means that about 90 % of the PV energy produced is directly used by the microgrid and 10% is injected to the main grid. This can be interpreted as the PVs being efficiently used or the PVs being undersized. Conversely, the SSI shows that the microgrid needs to rely on imported energy for more than half of its consumption.

In Fig. 8 three different case scenarios and their impact on the SCI and SSI are explored. These scenarios are: doubling the battery storage capacity, doubling the PVs kWp potential, and doubling both the battery storage capacity and kWp potential of each consumer respectively.

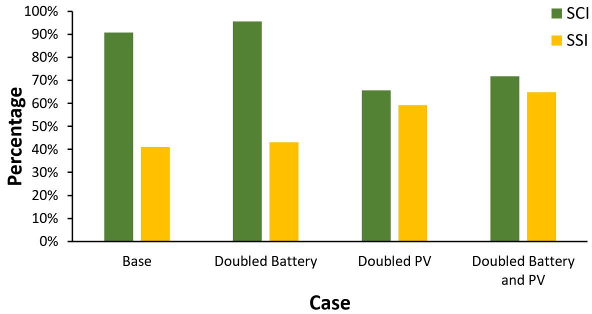

Fig. 8. Indexes comparison for different case scenarios

As shown in the results, increasing the ESS capacity has a minimal impact. Most of the PV energy was already being used. The increase in storage allows to store more, but not enough to significantly impact the SSI. The second case has a more significant influence on the SCI and SSI as shown in Fig. 8. The SSI is increased, but the SCI is greatly reduced. This is due to the lack of sufficient ESS to store all the energy being produced by the PVs. This can be seen in Fig. 9 as the exported energy in this case increases significantly. The final presented case shows a microgrid were both the PVs and ESS capacity has been doubled. As Fig. 9 shows, the increased storage capacity allows to reduce the amount of energy exported. This energy is instead stored and used by the DC microgrid thus preventing having to import energy from the main grid. As a consequence the saved energy increases in this case.

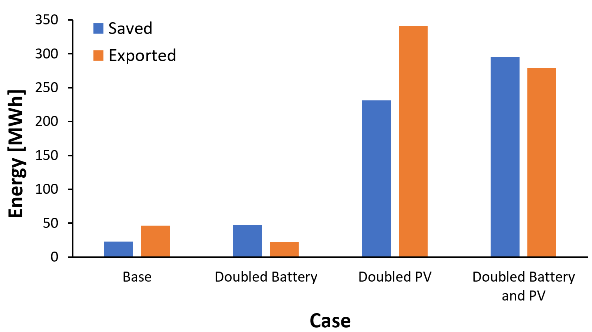

Fig. 9. Saved and exported energy in each case scenario

As previously shown, this tool allows to provide an insight to the possible obtainable results, and the impacts that changes on the configuration of the system can have on the saved energy. There are other factors that can affect this such as the consumption profiles themselves. Additionally, It is worth noticing that final changes have technical and economical constraints that have to be taken into account.

V. Conclusion

The presented approach allows to perform a steady state analysis of an industrial DC microgrid. The usage of the linear power flow allows for a flexible and fast calculation that allows to simulate constant power loads, non-dispatchable power sources, and dispatchable power sources. Through the use of sampled consumption data and irradiance data, a DC microgrid can be simulated for a specific duration of time. With this simulation, the expected performance of the microgrid can be calculated. This allows to evaluate important elements such as the needed line cross sections, expected currents, voltage evolution and expected energy savings. The results show a successful implementation of an example scenario and the types of results that can be obtained are demonstrated. Furthermore, the insights provided by the self-sufficiency and self-consumption index metrics were explored.

Future work could improve the versatility of the proposed approach by allowing to test different control methods. This would allow to compare their performance in terms of energy savings, currents, and voltage drops. The inclusion of weather and load forecasting to optimize the energy storage can also help further improve the versatility of the system.

References

[1] D. Kumar, F. Zare, and A. Ghosh, "DC Microgrid Technology: System Architectures, AC Grid Interfaces, Grounding Schemes, Power Quality, Communication Networks, Applications, and Standardizations Aspects," *IEEE Access*, vol. 5, pp. 12 230–12 256, 2017, read.

[2] H. Lotfi and A. Khodaei, "AC Versus DC Microgrid Planning," *IEEE Transactions on Smart Grid*, vol. 8, no. 1, pp. 296–304, Jan. 2017. [Online]. Available: http://ieeexplore.ieee.org/document/7225166/

[3] F. S. Al-Ismail, "DC Microgrid Planning, Operation, and Control: A Comprehensive Review," *IEEE Access*, vol. 9, pp. 36 154–36 172, 2021. [Online]. Available: https://ieeexplore.ieee.org/document/9366476/

[4] A. Maulik and D. Das, "Application of linearised load flow method for droop-controlled DCMGs," *IET Generation, Transmission & Distribution*, vol. 14, no. 6, pp. 1114–1126, Mar. 2020. [Online]. Available: https://digital-library.theiet.org/content/journals/10.1049/iet-gtd.2018.7113

[5] E. Vasquez Mayen and E. De Jaeger, "Linearised bipolar power flow for droop-controlled dc microgrids," in *2021 International Conference on Engineering and Emerging Technologies (ICEET)*, 2021, pp. 1–6.

[6] "Load flow simulation of a low-voltage pv-battery based dc micro-grid to supply small isolated communities," in *Proceedings of the 35th European Photovoltaic Solar Energy Conference and Exhibition*, ser. European Photovoltaic Solar Energy Conference and Exhibition (EU PVSEC). WIP Wirtschaft und Infrastruktur GmbH Co Planungs KG, Sep. 2018, pp. 1636–1640.

[7] J. M. Guerrero, J. C. Vasquez, J. Matas, L. G. De Vicuña, and M. Castilla, "Hierarchical control of droop-controlled AC and DC microgrids—A general approach toward standardization," *IEEE Transactions on industrial electronics*, vol. 58, no. 1, pp. 158–172, 2010, read.

[8] H. Azaioud, R. Claeys, J. Knockaert, L. Vandevelde, and J. Desmet, "A Low-Voltage DC Backbone with Aggregated RES and BESS: Benefits Compared to a Traditional Low-Voltage AC System," *Energies*, vol. 14, no. 5, p. 1420, Mar. 2021, read. [Online]. Available: https://www.mdpi.com/1996-1073/14/5/1420